

Sunspot Plume Observations in the EUV

The gas pressure differential between the umbra and surrounding region

J.G. Doyle¹ and M.S. Madjarska^{1,2}

¹ Armagh Observatory, College Hill, Armagh BT61 9DG, N. Ireland

² Mullard Space Science Laboratory, University College London, Holmbury St Mary, Dorking, Surrey RH5 6NT

....

Abstract. The electron density over a bright sunspot plume region was evaluated using lines within the O v 760 Å multiplet. The plume showed an intensity enhancement factor of ≈ 9 in the O v lines compared to regions outside the sunspot umbra. Internal agreement between the various ratios is excellent which would suggest that the O v lines do not suffer from blending problems. The derived mean electron densities for the sunspot plume is $\log N_e/cm^{-3} \approx 9.9$ compared to $\log N_e/cm^{-3} \approx 10.20-10.45$ in the surrounding area. The derived gas pressure in the plume compared to that outside leads weight to the suggestion that it is plasma flowing from outside the spot into the umbra at transition region temperatures that is the main cause of the down-flows. The plume non-thermal velocities are 5 to 10 km s⁻¹ smaller than those measured in regions external to the spot, suggesting significantly less turbulence within the umbra.

Key words. Sun: SoHO–SUMER: Transition region: Sunspot plumes: Electron density

1. Introduction

Sunspots, the cool dark features visible on the Sun’s surface are complex magnetic structures, perhaps even more so than previously considered as shown by recent high spatial resolution data (Scharmer et al. 2002). Based on SKYLAB data obtained in the mid-seventies, Foukal et al. (1974) and Noyes et al. (1985) showed the existence of plume features when viewed in lines formed around $1 - 2.5 \times 10^5$ K. These authors showed that lines formed around these temperatures were enhanced in radiance by factors up to 15–25 over the normal quiet Sun values. More recent work by Brynildsen et al. (2001) confirm these earlier studies and often show that these plume structures are largely dominated by down-flows of 20–30 km s⁻¹, similar to the earlier data reported by Dere (1982). From the dynamical viewpoint, this would suggest a pressure imbalance between the sunspot and the surrounding region. Although electron density estimates exist for sunspot plumes formed around 1×10^5 to 2.5×10^5 K (e.g. Doyle et al. 1985), none of these provide a comparison with data taken simultaneously in nearby structures outside of spots.

For a determination of the electron density, two such methods exist; line ratios and emission measure. Because structures in the transition region of the solar atmosphere are much less than the resolving power of any imaging experiment, estimates based on the emission measure are only lower limits to the true density. Thus the only accurate technique is the first, assuming

that the lines are from the same ion and that accurate atomic data exist for that particular ion. In this work we use data acquired with the SUMER instrument on-board SoHO taken around 760 Å.

This wavelength region includes the O v 760 Å multiplet. In ionization equilibrium, O v is formed at an approximate temperature of 2.5×10^5 K. Within this multiplet there are four line ratios, each using the 761.13 Å line. Here we use only three of these ratios due to blending in the fourth. All these lines are separated by less than 3 Å, thus this eliminates possible calibration uncertainties which can arise if the two lines have a large wavelength separation. In Sect. 2 we discuss the observational data, while Sect. 3 contains the results, including line width measurements.

2. Observational material

The *Solar Ultraviolet Measurements of the Emitted Radiation* (SUMER) instrument aboard the *Solar and Heliospheric Observatory* (SoHO) is a high resolution, stigmatic, normal incidence spectrometer covering the wavelength range from 660–1610 Å and 465–805 Å in first and second order, respectively (Wilhelm et al. 1995, 1997; Lemaire et al. 1997), with an angular pixel size in the direction along the slit of $\approx 1''$ and a spectral pixel size between 0.042–0.045 Å in first order. The dataset analysed in this paper was obtained on 18 March 1999, exposing a band of 120 spatial \times 1024 spectral pixels from detector B with a 0.3'' \times 120'' slit in first order, positioned through

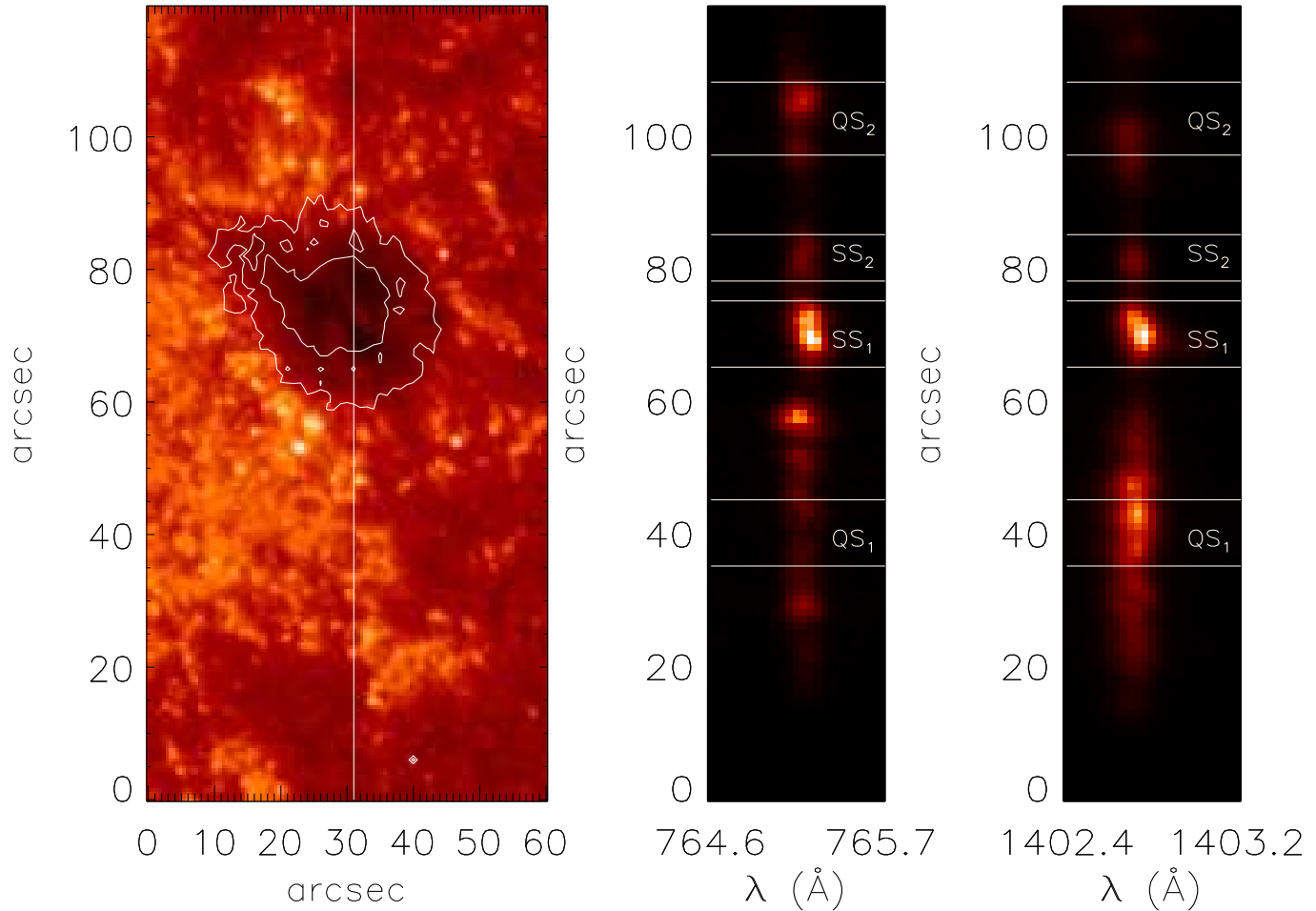


Fig. 1. A TRACE 1600 Å image of the sunspot and surrounding region (taken at 21:14 UT on 18 March 1999) with the position of the SUMER slit and TRACE white light contours over-plotted (left panel) out-lining the umbra and penumbra. The central panel and the right panel are the intensity variations along the SUMER slit as seen in N IV 765 Å (at 21:01 UT) and Si IV 1402.77 Å (at 20:13 UT) respectively. The 10'' region centered around 40'' along the slit is known as QS_1 , while QS_2 is the region centered around 100''. SS_1 and SS_2 are centered around 70'' and 80'' respectively along the slit.

the central part of a sunspot umbra. In Fig. 1, we show a TRACE 1600 Å image of the sunspot and surrounding region with the position of the SUMER slit and TRACE white light contours of the umbra/penumbra over-plotted. In the central panel of this figure is the intensity variation along the SUMER slit as seen in N IV 765 Å. The N IV 765 Å image shows enhanced emission over the sunspot umbra with $\approx 10''$ size which is identified as a plume area (SS_1). A better justification comes from the strong fbw registered in O IV and Si IV lines around 1400 Å an hour earlier. The down-fbw can also be seen in the N IV line, however it is smaller than that seen one hour earlier in Si IV.

In the quiet Sun, the O v lines are weak, however, the enhancement factor in the sunspot plume was ≈ 9 times higher than the mean intensity outside the sunspot. We should note as well that despite the fact that a rotational compensation has been applied, the SUMER slit moved $\approx 3.5''$ from its position where the 1400 Å spectrum was registered. Nevertheless, the plume remained in the SUMER field-of-view, but the fbw pattern changed either due to time variability or spatial location (we should return to this later).

Table 1. Line peak radiances in $Wsr^{-1}m^{-2}A^{-1}$ for the four selected regions (see text for details) for the six lines within the O v 760 Å multiplet.

Wavelength (Å)	QS_1	QS_2	SS_1	SS_2
758.68	0.115	0.121	1.117	0.63
759.43	0.104	0.100	0.853	0.482
760.21+760.43	0.384	0.403	3.563	1.98
761.13	0.028	0.041	0.179	0.087
761.99	0.119	0.139	1.105	0.602

The reduction of SUMER raw images involves local gain correction, flat-field subtraction and a correction for geometrical distortion. Since we only deal with lines from within the 760 Å multiplet (i.e. lines at 757.68, 759.43, 760.21, 760.43, 761.13 and 761.99 Å), the wavelength calibration derived from the header information is sufficient.

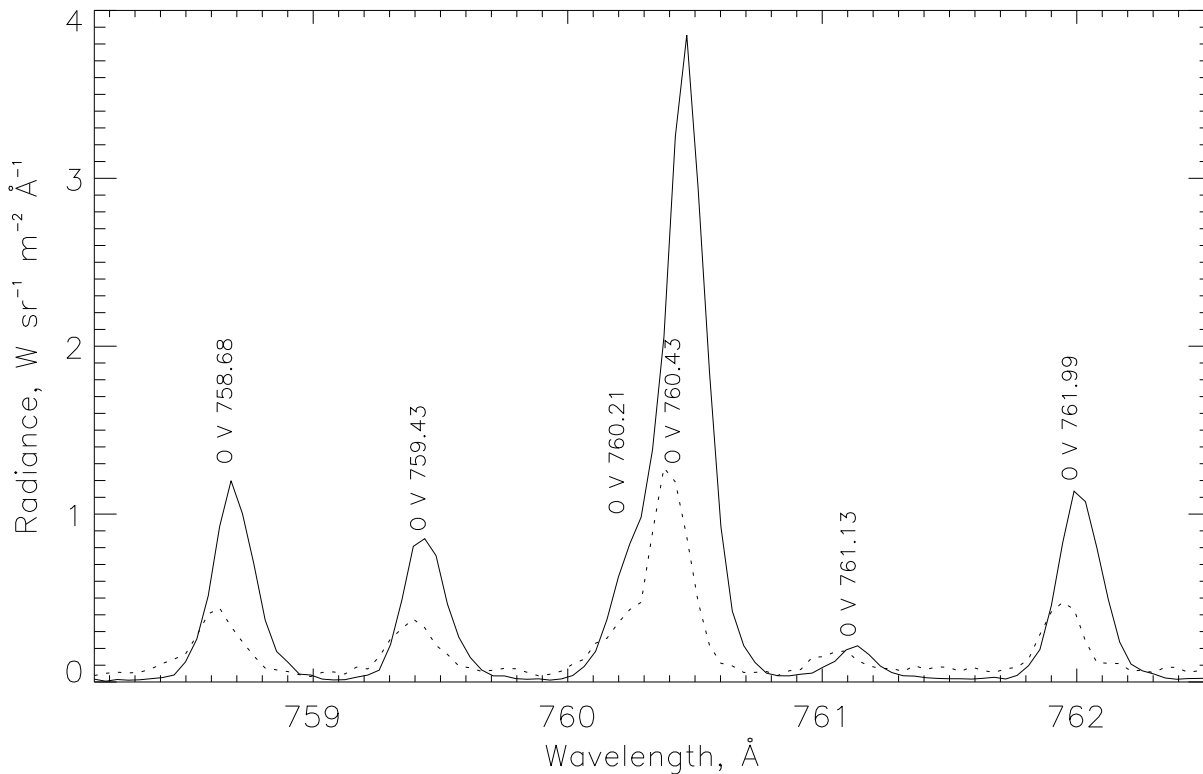


Fig. 2. The SUMER sunspot plume spectrum SS_1 (solid line) obtained on 18 March 1999 with the quiet sun QS_2 (dotted line) spectrum overplotted showing the six lines from within the O v 760 Å multiplet. Note that for presentation purposes the QS_2 spectrum was multiplied by a factor of three, also note the line-shift to the red in the sunspot data.

3. Results

Two regions within the sunspot and two regions outside the spot were selected for comparison. The sunspot plume spectra (SS_1) analysed here is shown in Fig. 2 with the quiet sun (QS_2) spectrum shown for comparison. Note the shift to the red in the sunspot data. In Table 1, we give the derived peak radiances in units of $Wsr^{-1}m^{-2}Å^{-1}$ for all four regions in each of the O v lines.

The electron density sensitivity of the various O v lines were evaluated using the contribution functions derived via CHIANTI (Young et al. 2003) and are shown in Fig. 3 (we did not include the blended 760.21/760.43 Å lines). All of these lines have a small electron temperature dependence as shown for one of the ratios in Fig. 4. For all the observed line ratios this translates into a possible error of no more than 20 %, which is within the accuracy of the atomic data.

An earlier paper by Wilhelm et al. (2002) suggested blending of the O v 759.43 Å line with a S iv line at 759.34 Å. However, as can be seen from Fig. 3, the internal agreement between the various ratios is excellent which would point to a negligible blending in any of the O v lines. The derived mean electron densities for the four regions are $\log N_e/cm^{-3} = 9.95, 9.88, 10.20$ and 10.45 for SS_1, SS_2, QS_1 and QS_2 respectively. Thus there is a clear factor of two or more difference between

the electron density in the sunspot umbra compared to the surrounding regions.

Based on the two strong unblended O v lines (758.68 and 759.43 Å), the FWHM values for the four regions, SS_1, SS_2, QS_1 and QS_2 (corrected for instrumental broadening) is 178, 152, 139 and 126 mÅ respectively. Assuming a line formation temperature of $\log T_e/K = 5.4$, this implies non-thermal velocities of 39, 32, 29 and 25 $km s^{-1}$ for the above four regions. Taking a slightly lower line formation temperature, e.g. $\log T_e/K = 5.3$ would increase the non-thermal velocities in the sunspot regions by 2 $km s^{-1}$. This could occur if large down-fbws were present. However, as noted above on examining several strong single resonance lines we did not obtain any evidence for fbws in excess of 20 $km s^{-1}$ at the time of the O v plume observations. As noted by Hansteen & Maltby (1992), a possible problem with any derived non-thermal velocities is the assumption that this additional component has a Gaussian distribution of velocities. It is beyond the scope of this paper to discuss this aspect.

4. Discussion

There are very few published results relating to electron density estimates in the mid-transition region for sunspots. Doyle et al. (1985) used several density sensitive line ratios on data obtained with an EUV spectrometer on-board SKYLAB. Si iii lines

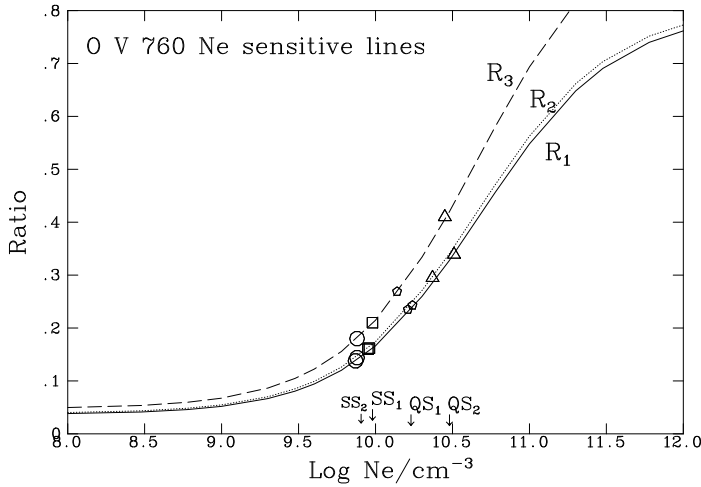


Fig. 3. Three electron density diagnostic line ratios from within the O v 760 Å multiplet, i.e. $R_1 = 761.13/758.68$, $R_2 = 761.13/759.43$ and $R_3 = 761.13/761.99$ plotted assuming the temperature of formation is $\log T_e/K = 5.4$. The derived densities (based on the data in Table 1) in all four regions are indicated.

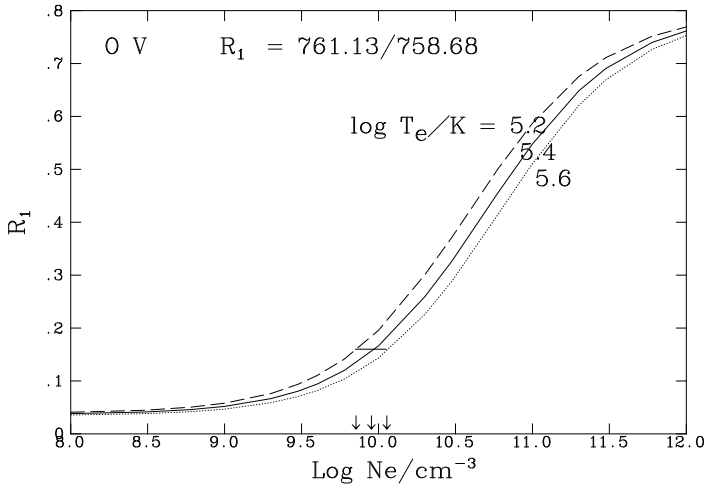


Fig. 4. The O v 761.13/758.68 line ratio for three different values of $\log T_e/K$; 5.2, 5.4 & 5.6, with the central temperature being the value at the peak of the O v contribution function. The short horizontal line is the SS1 line ratio while the arrows show the range of inferred electron densities.

(formed at $\log T_e/K \approx 4.5$) gives $N_e = 1 \times 10^{10} \text{cm}^{-3}$, C III lines (formed at $\log T_e/K \approx 4.8$) gives $N_e = 8 \times 10^9 \text{cm}^{-3}$, N IV lines (formed at $\log T_e/K \approx 5.0$) gives $N_e = 8 \times 10^9 \text{cm}^{-3}$ and finally O v lines implied $N_e = 1 \times 10^{10} \text{cm}^{-3}$. These observations were taken over a bright sunspot plume, similar to the SUMER data discussed here which implied $N_e = 9 \times 10^9 \text{cm}^{-3}$. The agreement between these two studies is excellent and although one may expect some variability, it is possible that sunspots showing bright plume structures may all have similar electron densities at transition region temperatures.

Brynildsen et al. (2001) showed the existence of red-shifted fbw channels from within the umbra of sunspots showing bright plumes to $50''$ – $60''$ outside the spot. In some instances, a

blue-shifted channel, smaller in size, was seen running parallel to the red-shifted material. As mentioned in Sect. 3, we did not find evidence for fbws in excess of 20 km s^{-1} during the time of the O v observations. However, data taken one hour earlier did show a fbw in excess of 80 km s^{-1} . Dere (1982), noted that fbws within sunspots can be very localized and since the width of the SUMER slit used here is only $0.3''$, coupled with the $3.5''$ shift between our N IV and Si IV observations, we may have missed the main fbw channel. On-the-other-hand, as noted by Brynildsen et al. (1998), these fbws can show changes on time-scales down to minutes.

The derived gas pressure in the plume compared to that outside the spot measured here would lead weight to the suggestion that it is plasma fbwing from outside the spot into the umbra at transition region temperatures that is the main cause of these down-fbws. Brynildsen et al. (2001) also noted that most plumes could be represented by a single Gaussian broadening by non-thermal motions, although in one spot, two fbws were observed, each with a width applying a zero non-thermal velocity. The non-thermal velocities derived here are 5 to 10 km s^{-1} smaller than those measured in regions external to the spot, suggesting significantly less turbulence within the umbra.

Acknowledgements. Research at Armagh Observatory is grant-aided by the N. Ireland Dept. of Culture, Arts and Leisure. This work was supported by PPARC grant PPA/GIS/1999/00055. The SUMER project is financially supported by DLR, CNES, NASA, and PRODEX. CHIANTI is a collaborative project involving NRL (USA), RAL (UK), and the Universities of Florence (Italy) and Cambridge (UK).

References

- Brynildsen, N., Brekke, P., Fredvik, T., et al. , 1998, *Sol Phys* 179, 279
 Brynildsen, N., Maltby, P., Fredvik, T., Kjeldseth-Moe, O. & Wilhelm, K., 2001, *Sol Phys* 198, 89
 Dere, K.P., 1982 *Sol Phys* 77, 77
 Doyle, J.G., Raymond, J.C., Noyes, R.W. & Kingston, A.E., 1985, *ApJ* 297, 816
 Foukal, P., Noyes, R.W., Reeves, E.M., et al. , 1974, *ApJ* 193, L143
 Hansteen, V. & Maltby, P., 1992, *Comm Astrophys* 16, 137
 Lemaire, P., Wilhelm, K., Curdt, W. et al. , 1997, *Sol Phys* 170, 105
 Noyes, R.W., Raymond, J.C., Doyle, J.G. & Kingston, A.E., 1985, *ApJ* 297, 805
 Scharmer, G.B., Gudiksen, B.V., Kiselman, D., et al. , 2002 *Nat* 420, 151
 Wilhelm, K., Curdt, W., Marsch, et al. , 1995, *Sol Phys* 162, 189
 Wilhelm, K., Lemaire, P., Curdt, W., et al. , 1997, *Sol Phys* 170, 75
 Wilhelm, K., Inhester, B. & Newmark, J.S., 2002, *A&A* 382, 328
 Young, P.R., Del Zanna, G., Landi, E., Dere, K.P., Mason, H.E. & Landini, M., 2003, *ApJ S* 144, 135